Rock Mech. Rock Engng. (2002) 35 (2), 95–108

Rock Mechanics and Rock Engineering

Numerical Analysis of Blast-Induced Stress Waves in a Rock Mass with Anisotropic Continuum Damage Models Part 2: Stochastic Approach

By

H. Hao[1], **C. Wu**[2], and **C. C. Seah**[3]

[1] Department of Civil and Resource Engineering, University of Western Australia, Crawley, Australia
[2] Protective Technology Research Center, Nanyang Technological University, c\o School of CEE, Singapore
[3] Defense Science and Technology Agency, Ministry of Defense, Singapore

Summary

This paper reports the second part of the study carried out by the authors on the underground explosion-induced stress wave propagation and damage in a rock mass. In the accompanying paper reporting the first part of the study, equivalent material properties were used to model the effects of existing cracks and joints in the rock mass. The rock mass and its properties were treated as deterministic. In this paper, existing random cracks and joints are modeled as statistical initial damage of the rock mass. In numerical calculation, an anisotropic continuum damage model including both the statistical anisotropic initial damage and cumulative damage dependent on principal tensile strain and stochastic critical tensile strain is suggested to model rock mass behavior under explosion loads. The statistical estimation of stress wave propagation in the rock mass due to underground explosion is evaluated by Rosenblueth's point estimate method. The suggested models and statistical solution process are also programmed and linked to Autodyn3D as its user's subroutines. Numerical results are compared with the field test data and those presented in the accompanying paper obtained with equivalent material property approach.

1. Introduction

The general behavior of a rock mass is usually anisotropic owing to naturally occurring network of flaws, joints and planes of weakness in it. Discontinuities such as cleavage cracks and defects involved in a rock mass can be characterized by their orientations, spacing, and number of discontinuities; and they have significant influence on the deformation and strength, stress wave propagation, and failure characteristics of a rock mass (Grady and Kipp, 1987). In order to estimate the effects of these discontinuities, much work has been done experimentally and theoretically on the description and calculation of behavior of a rock mass with cracks. For experimental study, King et al. (1986) measured the amplitudes and travel times of high frequency seismic stress waves which propagate parallel and perpendicular to columnar discontinuities in basalt, and noted lower particle velocities and greater high frequency attenuation in the direction perpendicular to the discontinuities than in the direction parallel to them. Many authors have also carried out analytical and numerical studies of rock discontinuity effects on stress wave propagation. In general, there are two approaches. One is to model the discontinuity by using discrete element method (Chen and Zhao, 1998; Hart, 1993) or block theory (Wang and Garga, 1993). And another is to examine the comprehensive effects of discontinuities by using the equivalent material properties of the rock mass (Kawamoto et al., 1988; Toi and Atluri, 1990; Taylor et al., 1986; Yang et al., 1996; Liu and Katsabanis, 1997). Usually the first method is used to model a few large discontinuities, while the second approach is adopted when the discontinuities are dense and have uncertain properties.

Recently, a few researchers used theory of continuum damage mechanics on modelling rock mass responses to either static or dynamic loads (Hao et al., 1998; Wu et al., 1999; Zhang and Valliappan, 1990b; Zhang and Valliappan, 1998a,b). In these studies, the discontinuities in the rock mass are modelled as initial damage before loading. Wu et al. (2000) used the P and S wave velocities measured at the granite site under consideration in a field seismic survey to derive a statistical isotropic initial damage model for the rock mass. They subsequently applied the statistical initial damage model in a stochastic analysis of isotropic rock damage to underground blasting loads (Wu et al., 1999). Although reasonably good predictions of the stress wave propagation and rock damage were achieved in that study, the assumption of isotropic damage of the rock mass can be further improved. This is because discontinuities in a rock mass normally show some predominant orientations although the distributions of flaws and cracks in space, their size and orientations are basically random. This phenomenon makes the initial damage anisotropy. In addition, the isotropic measure of damage is unable to account for the dynamic change in direction of the maximum damage distribution relative to that of the maximum principal tensile strain, especially in cases where nonproportionality in strain histories is present. Sometimes even though the rock mass is initially isotropic, its behavior may change to anisotropy during a damage process. Thus it is necessary to develop a random anisotropic damage model to analyze blasting-induced stress waves in a rock mass.

The first anisotropic initial damage model for the rock mass was suggested by Kawamoto et al. (1988). They counted the number of cracks, measured directions and cross-section area of the cracks in a 15 m $\times$ 15 m $\times$ 15 m rock specimen sampled from a rock mass, and used the concept of damage mechanics to derive the initial damage of the rock mass. Zhang and Valliappan (1990a) used the data reported by Kawamoto et al. (1988) to derive a statistical initial damage for the rock mass. It was found that the statistical initial damage obeys a beta distribution. They subsequently used that statistical initial damage model in analyzing a rock slope stability (Zhang and Valliappan, 1990b). In the later study, however, anisotropic damage evolution and propagation were not considered. Recently, Swoboda et al. (1998) also derived an anisotropic initial damage model for a rock mass by measuring the existing crack sets in it. Based on the field and laboratory measured data, a statistical anisotropic initial damage model and statistical material properties of the granite mass at the site under study were derived by the authors (Wu et al., 2001). It was found that the anisotropic initial damage also obeys beta distributions, anisotropic elastic moduli follow normal distributions.

In this paper, an anisotropic constitutive model with statistical initial damage and cumulative damage is presented to model rock damage resulting from impulsive loading. The statistical initial damage and material properties derived earlier (Wu et al., 2001) are used here. The randomness of the initial damage, which relates to the elastic and shear modulus, and the randomness of critical tensile strain, which relates to the rock material stiffness and strength degradation, are included in numerical calculations. The variations of other parameters, such as the material constant α_i, the mass density, and Poisson's ratio are, however, neglected as they have little effects on the response of a rock mass under dynamic loading (Yang et al., 1996). The statistical estimation of stress wave propagation and damage in the rock mass due to underground explosion is evaluated by the Rosenblueth's point estimate method (1975, 1981).

The present statistical damage model has also been implemented in Autodyn3D (1997) as its user defined subroutines. The numerical results of peak particle velocities and peak particle accelerations obtained by the Rosenblueth's point estimate method (1975, 1981) are compared with those obtained by using deterministic method with equivalent material properties in Part I as well as the field measured data. The effects of statistical variations of anisotropic initial damage and critical tensile strain of the rock mass on their dynamic responses and damage zones are discussed.

2. Anisotropic Damage Model and Constitutive Law

Because initial damage exists in the rock mass, the stiffness of the rock mass is reduced before loading. Under dynamic loading, the initial damage will evolve and propagate and new ones will be generated. In the accompanying paper (Hao et al., 2002), only anisotropic cumulative damage is defined while the effects of anisotropic initial damage are considered by using equivalent material properties. In this paper, cumulative damage is assumed to evolve from statistical initial damage. If the maximum tensile strain is less than the stochastic critical strain ε_{cri}, there is only initial damage D_i^s in the rock mass. If the maximum tensile strain exceeds ε_{cri}, the material properties will continue to degrade with the cumulative damage. Thus, the damage variable of the rock mass per volume V_0 under explosion loads, which includes both the initial damage and cumulative damage, is then

$$\begin{aligned} D_i(D_i^s, \varepsilon_{cri}, \varepsilon_i, t) &= 1 - (1 - D_i^s)(1 - D_i^d(t)) \\ &= 1 - (1 - D_i^s)\exp[-\alpha_i(\varepsilon_i - \varepsilon_{cri})^{\beta_i} V_0 t], \end{aligned} \tag{1}$$

where $D_i^d(t)$ is cumulative damage whose definition is similar to that derived in the accompanying paper (Hao et al., 2002) except it is a stochastic number depending on the statistical variations of ε_{cri}; D_i^s is the anisotropic initial damage in the rock mass.

3. Statistical Estimation of Damage Material Properties Under Consideration

The site under consideration consists of a quarry site with mainly unweathered granite. A detailed geological investigation which includes seismic surveys, visual inspection of rock mass, deep coring, color TV imaging and impression packer tests in boreholes, had been carried out due to some underground construction activities (Soil and Foundation Ltd., 1996). Much information about the properties of the granite has been provided by the investigations and survey studies. The data from the investigations were used in a statistical analysis of the properties of the rock mass in a previous study (Wu et al., 2001). Owing to the random distributions of cracks in a rock mass in sizes, directions and spacing, the properties of rock mass need to be evaluated by using the methods of statistical analysis. In a previous study (Wu et al., 2001), a three-dimensional geometric model of cracks has been established in terms of the statistical orientations, spacing and normalized size of cracks in the rock mass based on the field and laboratory data (Soil and Foundation Ltd., 1996). The definition of damage tensor for one crack is given by the following equation (Wu et al., 2001):

$$[D] = \omega \begin{bmatrix} n_1 n_1 & n_1 n_2 & n_1 n_3 \\ n_2 n_1 & n_2 n_2 & n_2 n_3 \\ n_3 n_1 & n_3 n_2 & n_3 n_3 \end{bmatrix}, \tag{2}$$

in which $\mathbf{n} = [l, m, n]^T$ is the direction vector of damage tensor D of the crack plane, and ω is the characteristic damage value which is based on the length, spacing, dip, and dip direction of cracks on rock specimens. The dip, dip direction, spacing, and normalized size of cracks of the granite were obtained from cores. Based on the model, probabilistic distribution laws of geometric parameters of cracks at the granite site were derived. The distribution of anisotropic initial damage of the granite mass is derived and found having a beta distribution according to these statistical distributions and using Monte-Carlo simulation method based on Eq. (2). It is found that the mean and standard deviation of initial damage in three directions in the rock mass are $\mu(D_1^s) = 0.162$, $\sigma(D_1^s) = 0.091$, $\mu(D_2^s) = 0.124$, $\sigma(D_2^s) = 0.069$, and $\mu(D_3^s) = 0.222$, $\sigma(D_3^s) = 0.122$, respectively, where 1, 2, and 3 indicate radial, lateral and vertical $(x, y\ z)$ directions as defined by Hao et al., (2002). The initial damage variable D_i^s was found to have the beta distribution with probability density function and cumulative distribution function

$$f(D_i^s) = \frac{1}{B(a_i, b_i)} D_i^{s\,a_i-1} (1 - D_i^s)^{b_i-1} \tag{3}$$

and

$$F(D_i^s) = \frac{1}{B(a_i, b_i)} \int_0^{D_i^s} x^{a_i-1} (1-x)^{b_i-1}\, dx, \tag{4}$$

where a_i is a parameter of size; b_i is a parameter of shape; $B(a_i, b_i)$ is the beta function and

$$B(a_i, b_i) = \int_0^1 x^{a_i-1} (1-x)^{b_i-1}\, dx. \tag{5}$$

For the site under consideration, it has $a_1 = 2.49$, $b_1 = 12.90$, $a_2 = 2.71$, $b_2 = 19.11$, and $a_3 = 2.35$, $b_3 = 8.25$ (Wu et al., 2001).

Based on the laboratory test data (Soil and Foundation Ltd., 1996), a previous study also found the damaged elastic modulus of the site having a normal distribution with mean $\mu(E) = 73.9$ GPa and standard deviation $\sigma(E) = 12.14$ GPa; and static tensile strength σ_{sti} follows a gamma distribution with $k = 69.7$ and $\lambda = 3.99$ (Wu et al., 2000). In the present study, the elastic modulus of the undamaged rock material is estimated by the 95 percentile confidence level as $\mu(E) + 1.645\sigma(E) = 93.87$ GPa.

Because damage is dependent on the critical tensile strain, and critical tensile strain in three principal directions can be estimated by

$$\varepsilon_{cri} = \sigma_{sti}/E(1 - D_i^s)^2. \tag{6}$$

Using the statistical distributions of σ_{sti} and D_i^s, statistical data of ε_{cri} can be obtained by Monte-Carlo simulation. Simulated results in this paper indicate that the probability distribution of random critical tensile strain ε_{cri} has a normal distribution

$$f(\varepsilon_{cri}) = \frac{1}{\sigma(\varepsilon_{cri})\sqrt{2\pi}} e^{-(\varepsilon_{cri}-\mu(\varepsilon_{cri}))^2/(2\sigma^2(\varepsilon_{cri}))}, \tag{7}$$

with mean and standard deviation equal to $\mu(\varepsilon_{cr1}) = 0.265 \times 10^{-3}$ and $\sigma(\varepsilon_{cr1}) = 0.068 \times 10^{-3}$, $\mu(\varepsilon_{cr2}) = 0.253 \times 10^{-3}$ and $\sigma(\varepsilon_{cr2}) = 0.048 \times 10^{-3}$, and $\mu(\varepsilon_{cr3}) = 0.307 \times 10^{-3}$ and $\sigma(\varepsilon_{cr3}) = 0.109 \times 10^{-3}$, respectively. Those normal distributions are examined by the method of Kolmogorov-Smirnov statistical goodness-of-fit test with a confidence level of 95%, indicating a good fit of the distribution function to the simulated data.

According to the damage definition given in Eq. (1), there are two random variables, namely, the initial anisotropic damage D_i^s and critical tensile strain ε_{cri}. Based on the Rosenblueth's method, mean and standard deviation of anisotropic damage variable can be obtained by

$$\{\mu(D_i)\}_{D_i^s,\varepsilon_{cri}} = \frac{1}{4}(\{D_i\}^{++} + \{D_i\}^{--} + \{D_i\}^{+-} + \{D_i\}^{-+}) \tag{8}$$

$$\{\sigma^2(D_i)\}_{D_i^s,\varepsilon_{cri}} = \{\mu(D_i^2)\} - \{\mu^2(D_i)\}, \tag{9}$$

where

$$\{D_i\}^{\pm\pm} = \{D_i(\mu(D_i^s) \pm \sigma(D_i^s), \mu(\varepsilon_{cri}) \pm \sigma(\varepsilon_{cri}), \varepsilon_i, t\}. \tag{10}$$

The estimators of mean and standard deviation of damaged material properties E_i^*, v_{ij}^* and G_{ij}^* are then

$$\mu(E_i^*) = E_i[1 - \sigma(D_i)]^2 + E_i\sigma^2(D_i) \tag{11}$$

$$\sigma(E_i^*) = E_i[1 - \sigma(D_i)]\sigma(D_i) \tag{12}$$

$$\mu(v_{ij}^*) = v_{ij}\frac{[1 - \sigma(D_i)][1 - \sigma(D_j)]}{[1 - \sigma(D_j)]^2 - \sigma^2(D_j)} \quad i \neq j \tag{13}$$

$$\sigma(v_{ij}^*) = v_{ij}\frac{\{[1 - \sigma(D_i)]^2\sigma^2(D_j) + [1 - \sigma(D_j)]^2\sigma^2(D_i)\}^{1/2}}{[1 - \sigma(D_j)]^2 - \sigma^2(D_j)} \quad i \neq j \tag{14}$$

$$\mu(G_{ij}^*) = \frac{1}{2} G_{ij}(\Delta_{ij}^{++} + \Delta_{ij}^{+-} + \Delta_{ij}^{-+} + \Delta_{ij}^{--}) \tag{15}$$

$$\begin{aligned}\sigma(G_{ij}^*) = G_{ij}\{&[(\Delta_{ij}^{++})^2 + (\Delta_{ij}^{+-})^2 + (\Delta_{ij}^{-+})^2 + (\Delta_{ij}^{--})^2] \\ &- \frac{1}{4}[\Delta_{ij}^{++} + \Delta_{ij}^{+-} + \Delta_{ij}^{-+} + \Delta_{ij}^{--}]^2\}^{1/2},\end{aligned} \tag{16}$$

where

$$\Delta_{ij}^{\pm\pm} = \frac{\{[1-\mu(D_i)] \pm \sigma(D_i)\}^2 \{[1-\mu(D_j)] \pm \sigma(D_j)\}^2}{\{[1-\mu(D_i)] \pm \sigma(D_i)\}^2 + \{[1-\mu(D_j)] \pm \sigma(D_j)\}^2}. \tag{17}$$

Based on the Rosenblueth's point estimate method (see appendix A Eqs. (A13)–(A17)), the expected matrix and standard deviation matrix corresponding to the damaged anisotropic constitutive relation as given in the accompanying paper (Hao et al., 2002) can be derived as

$$\mu(S_{ij}^*) = S_{ij} \frac{[1-\mu(D_i)][1-\mu(D_j)] + \sigma(D_i)\sigma(D_j)\delta_{ij}}{\{[1-\mu(D_i)]^2 - \sigma^2(D_i)\}\{[1-\mu(D_j)]^2 - \sigma^2(D_j)\}^2} \quad i,j = 1,2,3 \tag{18}$$

$$\begin{aligned}&\sigma(S_{ij}^*) = S_{ij} \\ &\times \frac{\{(1+\delta_{ij})\{[1-\mu(D_i)]^2\sigma^2(D_i) + [1-\mu(D_j)]^2\sigma^2(D_j)\} + \sigma^2(D_i)\sigma^2(D_j)(1-\delta_{ij})\}^{1/2}}{\{[1-\mu(D_i)]^2 - \sigma^2(D_i)\}\{[1-\mu(D_j)]^2 - \sigma^2(D_j)\}^2} \\ &\quad i,j = 1,2,3,\end{aligned} \tag{19}$$

where $\delta_{ij} = 0$ for $i \neq j$ and $\delta_{ij} = 1$ for $i = j$.

$$\mu(S_{44}^*) = S_{44}\left\{\frac{[1-\mu(D_2)]^2 + \sigma^2(D_2)}{\{[1-\mu(D_2)]^2 - \sigma^2(D_2)\}} + \frac{[1-\mu(D_3)]^2 + \sigma^2(D_3)}{\{[1-\mu(D_3)]^2 - \sigma^2(D_3)\}}\right\} \tag{20}$$

$$\sigma(S_{44}^*) = 2S_{44}\left\{\frac{[1-\mu(D_2)]^2\sigma^2(D_2)}{\{[1-\mu(D_2)]^2 - \sigma^2(D_2)\}} + \frac{[1-\mu(D_3)]^2\sigma^2(D_3)}{\{[1-\mu(D_3)]^2 - \sigma^2(D_3)\}}\right\}^{1/2} \tag{21}$$

$$\mu(S_{55}^*) = S_{55}\left\{\frac{[1-\mu(D_3)]^2 + \sigma^2(D_3)}{\{[1-\mu(D_3)]^2 - \sigma^2(D_3)\}} + \frac{[1-\mu(D_1)]^2 + \sigma^2(D_1)}{\{[1-\mu(D_1)]^2 - \sigma^2(D_1)\}}\right\} \tag{22}$$

$$\sigma(S_{55}^*) = 2S_{55}\left\{\frac{[1-\mu(D_3)]^2\sigma^2(D_3)}{\{[1-\mu(D_3)]^2 - \sigma^2(D_3)\}} + \frac{[1-\mu(D_1)]^2\sigma^2(D_1)}{\{[1-\mu(D_1)]^2 - \sigma^2(D_1)\}}\right\}^{1/2} \tag{23}$$

$$\mu(S_{66}^*) = S_{66}\left\{\frac{[1-\mu(D_1)]^2 + \sigma^2(D_1)}{\{[1-\mu(D_1)]^2 - \sigma^2(D_1)\}} + \frac{[1-\mu(D_2)]^2 + \sigma^2(D_2)}{\{[1-\mu(D_2)]^2 - \sigma^2(D_2)\}}\right\} \tag{24}$$

$$\sigma(S_{66}^*) = 2S_{66}\left\{\frac{[1-\mu(D_1)]^2\sigma^2(D_1)}{\{[1-\mu(D_1)]^2 - \sigma^2(D_1)\}} + \frac{[1-\mu(D_2)]^2\sigma^2(D_2)}{\{[1-\mu(D_2)]^2 - \sigma^2(D_2)\}}\right\}^{1/2}. \tag{25}$$

4. Statistical Dynamic Response Analysis

In statistical analysis, the upper and lower limit states of damage can be estimated by

$$\mu(D_1) \pm \sigma(D_1); \quad \mu(D_2) \pm \sigma(D_2); \quad \mu(D_3) \pm \sigma(D_3); \tag{26}$$

The upper and lower limit damage states are associated with the larger and smaller stiffness loss. The upper and lower limit states of damaged stiffness may be evaluated by

$$[K_{ij}(D)]^{\pm\pm\pm} = [K_{ij}(\mu(D_1) \pm \sigma(D_1), \mu(D_2) \pm \sigma(D_2), \mu(D_3) \pm \sigma(D_3))] \tag{27}$$

where $[K_{ij}(D)]^{+++}$ is the upper limit state of damaged stiffness; and $[K_{ij}(D)]^{---}$ is the lower limit state of damaged stiffness.

It can be noted that if the stiffness is in the upper limit state, the displacement should be smaller. It will be larger if stiffness is in the lower limit state. By using Eq. (1) in the accompanying paper (Hao et al., 2002) with different combinations of damaged stiffness matrix, the corresponding displacements $\{u\}^{+++}$, $\{u\}^{++-}, \ldots, \{u\}^{---}$ can be obtained.

Based on the Rosenblueth's method, the mean and variance of displacements corresponding to the mean and mean plus or minus standard deviation of initial damage and critical tensile strain can be expressed as

$$\{\mu(U)\}_{D_1,D_2,D_3} = \frac{1}{8}(\{U\}^{+++} + \{U\}^{++-} + \cdots + \{U\}^{---}) \tag{28}$$

$$\{\sigma^2(U)\}_{D_1,D_2,D_3} = \{\mu(U^2)\} - \{\mu^2(U)\}. \tag{29}$$

5. Numerical Results

To demonstrate the statistical method presented in the previous sections, the same field blasting tests at the granite site as presented by Hao et al. (2002) are simulated.

Figure 1 shows the comparisons of the calculated mean peak particle velocities (PPV) and the peak particle accelerations (PPA) in the rock mass (free field) at different scaled distances in the Y direction by two different methods. The thin line shows the response values obtained by using the equivalent material properties, whereas the bold dotted line shows the mean responses calculated by using Rosenblueth's method. The corresponding best fitted curves of the field measured data in the Y direction are also shown for comparison in the figure. As shown in the figure, the differences for PPV between the numerical results obtained by statistical approach and deterministic approach are not significant. It also shows that the results for PPA from the statistical analysis have similar slope as the field measured data, whereas those from the deterministic approach display a more rapid attenuation with the scaled distance. Considering the many uncertainties involved in the explosion process and rock mass, numerical results, simulated by both deterministic and statistical methods are reasonably good. However, it seems that the statistical approach gives relatively better prediction of PPA. This is probably because it considers the effects of existing cracks and discontinuities in the rock mass in a more sophisticated way than using the equivalent material properties.

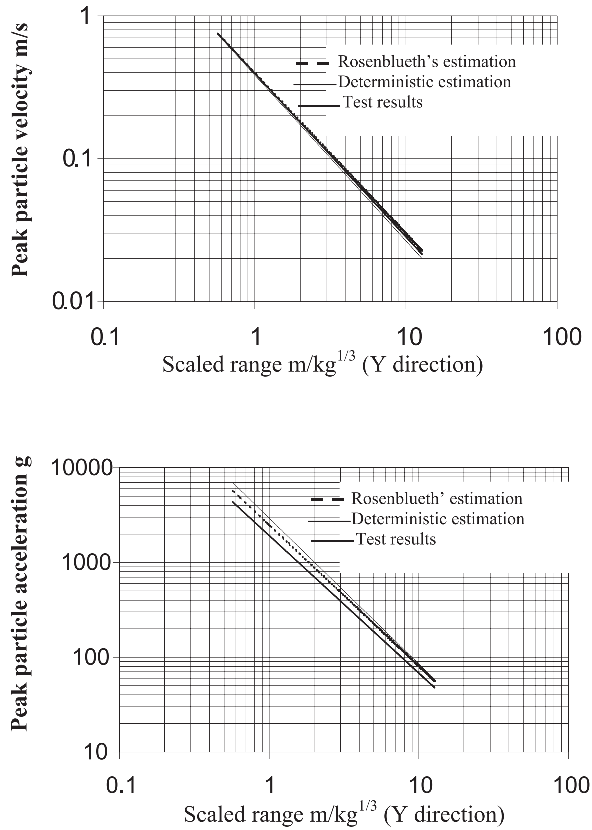

Fig. 1. Comparisons of attenuation of PPV and PPA in the Y direction

Figure 2 shows the calculated mean damage zone around the charge hole in the rock mass using Rosenblueth's method when charge weight is 50 kg. It should be noted that the critical damage value of 0.632 suggested by Liu and Katsabanis (1997) considers only the evaluated damage due to external loading, whereas the damage value shown in the figure includes the accumulated damage, i.e., initial damage and damage evolution owing to blasting loads. If the critical evolutionary damage value of 0.632 is assumed, the critical accumulated damage can be estimated by Eq. (1). Using the mean initial damage values, the estimated critical values in the three directions are $D_{c1} = 0.69$, $D_{c2} = 0.68$ and $D_{c3} = 0.71$, respectively. When damage value shown in the figure is larger than those critical values, the rock mass is considered failed. As shown in the figure, the intensive damage zone extends in the X direction 1.32 m, Y direction 1.18 m and no intensive damage of rock mass in the vertical direction due to the cylindrical shape charge hole. The damage zone in the X direction is larger than that in the Y direction because the X direction has more significant initial damage as discussed above. It should also be noted that the intensive damage zones estimated by the present model are deeper

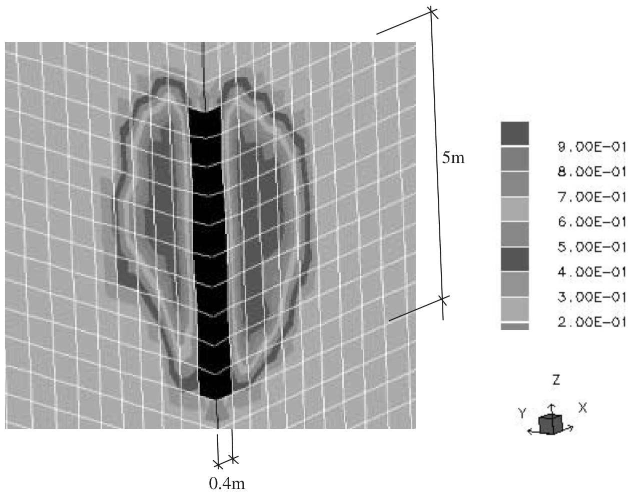

Fig. 2. Distribution of damage variable D around the charge hole (charge weight 50 kg)

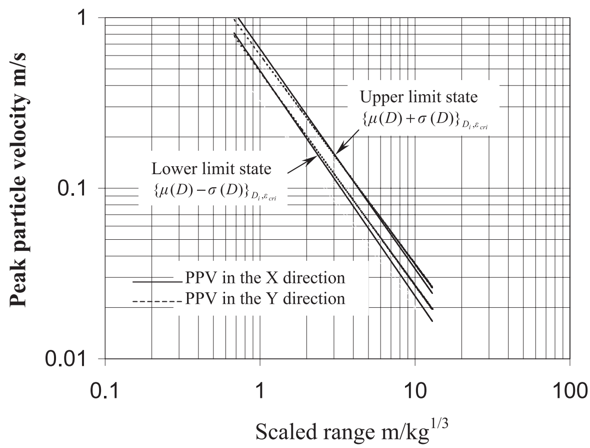

Fig. 3. Upper and lower limit states of PPV in the X and Y directions

into the rock mass in both the X and Y directions as compared to those assessed in the accompanying paper (Hao et al., 2002).

One advantage of conducting statistical analysis is that it allows probabilistic confidence estimation of the responses besides the mean responses. Figure 3 shows the estimated attenuation PPV curves obtained with $\{\mu(D) \pm \sigma(D)\}_{D_i,\varepsilon_{cri}}$ in both the X and Y directions. As shown, the responses in both directions corresponding to the mean minus and plus one standard deviation differ by about 30%.

Figure 4 shows the estimated attenuation PPA curves obtained with $\{\mu(D) \pm \sigma(D)\}_{D_i,\varepsilon_{cri}}$. It shows that the lower (mean minus one standard deviation) and upper (mean plus one standard deviation) limit responses in the X and Y directions obtained by considering the statistical variations differ by about 25%.

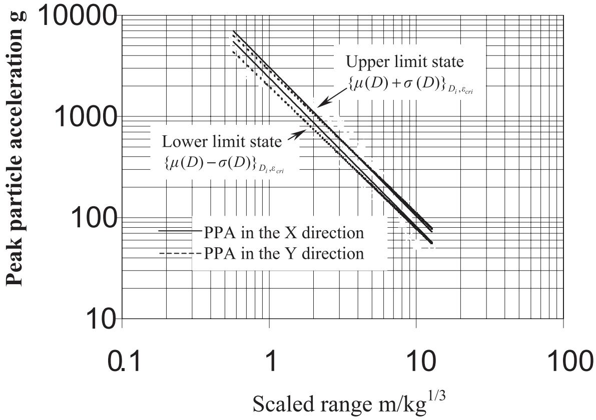

Fig. 4. Upper and lower limit states of PPA in the X and Y directions

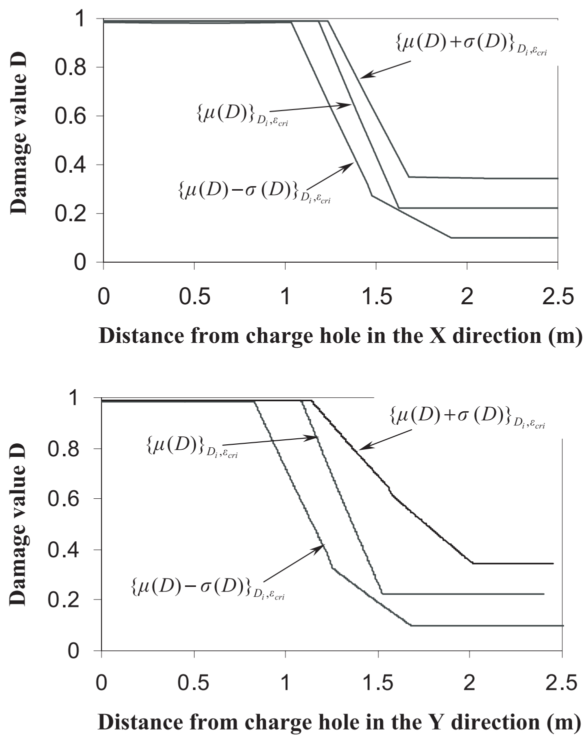

Fig. 5. Estimated damage value along a horizontal plane in the rock mass corresponding to $\{u(D)\}_{D_i,\varepsilon_{cri}}$ and $\{\mu(D) \pm \sigma(D)\}_{D_i,\varepsilon_{cri}}$ in the X and Y directions (charge weight 50 kg)

Figure 5 shows a comparison of the calculated damage along a horizontal plane in both the X and Y directions at the same depth as the explosive in the rock mass under $\{\mu(D)\}_{D_i,\varepsilon_{cri}}$ and $\{\mu(D) \pm \sigma(D)\}_{D_i,\varepsilon_{cri}}$ when charge weight is 50 kg. It should be noted that the initial mean damage, initial mean plus and minus one

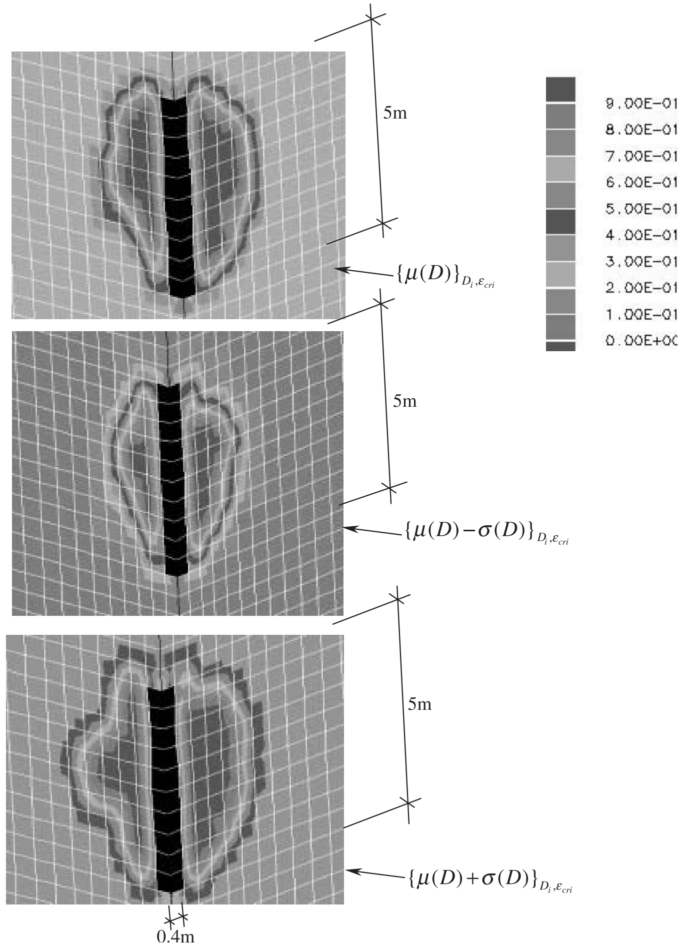

Fig. 6. Damage zone in the rock mass around the charge hole under $\{\mu(D)\}_{D_i,\varepsilon_{cri}}$ and $\{\mu(D) \pm \sigma(D)\}_{D_i,\varepsilon_{cri}}$ (charge weight 50 kg)

standard deviation damage in the X direction are respectively 0.162, 0.251 and 0.071, and those in the Y direction are 0.124, 0.193 and 0.055. It should also be noted that the maximum damage values around the charge hole are calculated to be 1.0 indicating excessive damage in the rock mass around the charge hole. The intensive damage zones, say 0.69 and 0.68 in the X and Y directions, under mean, mean minus and mean plus one standard deviation, are respectively about 1.32 m, 1.51 m and 1.21 m deep into the rock mass in the X direction, and 1.18 m, 1.42 m and 1.01 m deep into the rock mass in the Y direction. It should be noted that these values only indicate that rock mass has lost its stiffness by about 68%, whereas the exact depth of crack extension into the rock mass is not known. The respective damage zones generated in the rock mass corresponding to the above three cases are shown in Fig. 6.

6. Conclusions

This paper presents a statistical method to analyze stochastic stress wave propagation and damage zones generated in a rock mass due to underground explosion. It models the existing discontinuities in the rock mass as statistical anisotropic initial damage. The statistical anisotropic critical tensile strain is also included in the model. The anisotropic statistical damage of rock mass under dynamic loading is accumulated from the statistical initial damage. The results of numerical analysis indicate that the method of combining the statistical initial damage and dynamic damage evolution can predict not only the stress wave intensities in a rock mass, but also give a range of lower and upper limit states of peak values of stress wave. It also estimates the lower and upper limit of damage zones generated by the explosion in the rock mass. Although field observation indicates the reasonableness of the numerically estimated damage zones, more accurate calibration is necessary by actually measuring the generated damage zone in the rock mass after blasting tests.

References

Autodyn3D (1997): AUTODYN User Manual, Revision 3.0. Century Dynamics, San Ramon, CA.

Chen, S. G., Zhao, J. (1998): A study on UDEC modelling of blast wave propagation in jointed rock mass. Int. J. Rock Mech. Min. Sci. 35, 93–99.

Grady, D. E., Kipp, M. E. (1987): Dynamic rock fragmentation, In: Atkinson, B. K. (ed.) fracture mechanics of rock, Chapter 10. Academic Press, London, 429–475.

Hao, H., Ma, G. W., Zhou, Y. X. (1998): Numerical simulation of underground explosions. Fragblast, Int. J. Blasting Fragment. 2, 383–395.

Hao, H., Wu, C., Zhou, Y. X. (2002): Numerical analysis of blasting-induced stress wave in anisotropic rock mass with continuum damage models. Part I: Equivalent material property approach. Rock Mech. Rock Engng. 35(2).

Hart, R. D. (1993): An introduction to distinct element modelling for rock engineering. In: Hudson, J. A. (ed.) Comprehensive rock engineering, vol. 2, Pergamon Press, Oxford, 245–261.

Kawamoto, T., Ichikawa, Y., Kyoya, T. (1988): Deformation and fracturing behaviour of discontinuous rock mass and damage mechanics theory. Int. J. Numer. Anal. Met. Geomech. 12, 1–30.

King, M. S., Myer, L. R., Rezowalli, J. J. (1986): Experimental studies of elastic-waves propagation in a columnar-jointed rock mass. Geophys. Prospecting 34, 1185–1199.

Liu, L., Katsabanis, P. D. (1997): Development of a continuum damage model for blasting analysis. Int. J. Rock Mech. Min. Sci. 34, 217–231.

Rosenblueth, E. (1975): Point estimates for probability moments. Proc., Natl. Acad. Sci. U. S. A. 72, 3812–3814.

Rosenblueth, E. (1981): Two-point estimates in probability. Appl. Math. Model. 5, 329–335.

Soil and Foundation Ltd. (1996): Seismic survey and site investigation works at Mandai for Lands and Estates Organization, Ministry of Defence. Vol. I, Site investigation. Ministry of Defence, Singapore.

Swoboda, G., Shen, X. P., Rosas, L. (1998): Damage model for jointed rock mass and its application to tunnelling. Computers Geotechnics 22(34), 183–203.

Taylor, L. M., Chen, E. P., Kuszmaul, J. S. (1986): Micro-crack induced damage accumulation in brittle rock under dynamic loading. Computer Meth. Appl. Mech. Eng. 55, 301–320.

Toi, Y., Atluri, S. N. (1990): Finite element analysis of static and dynamic fracture of brittle micro-cracking solids. Int. J. Plasticity 6, 389–414.

Wang, B. L., Garga, V. K. (1993): A numerical method of modelling large displacements of jointed rocks. Part I: Fundamentals. Can. Geotech. J. 30, 96–108.

Wu, C., Hao, H., Zhou, Y. (1999): Dynamic response analysis of rock mass with stochastic properties subjected to explosive loads. Fragblast, Int. J. Blasting Fragment. 3, 137–153.

Wu, C., Hao, H., Zhou, Y. X. (2000): Statistical properties of the Bukit Timah Granite in Singapore. J. Testing Evaluation ASTM 28(1), 36–43.

Wu, C., Hao, H., Zhao, J., Zhou, Y. X. (2001): Statistical analysis of anisotropic damage of the Bukit Timah Granite. Rock Mech. Rock Engng. 34(1), 23–38.

Yang, R., Bawden, W. F., Katsabanis, P. D. (1996): A new constitutive model for blast damage. Int. J. Rock Mech. Min. Sci. Geomech. Abstr. 33, 245–254.

Zhang, W., Valliappan, S. (1990a): Analysis of random anisotropic damage mechanics problems of rock mass, Part I: Probabilistic analysis. Rock Mech. Rock Engng. 23, 91–112.

Zhang, W., Valliappan, S. (1990b): Analysis of random anisotropic damage mechanics problems of rock mass, Part II: Statistical estimation. Rock Mech. Rock Engng. 23, 241–259.

Zhang, W., Valliappan, S. (1998a): Continuum damage mechanics theory and application, Part I: Theory. Int. J. Damage Mech. 7, 250–273.

Zhang, W., Valliappan, S. (1998b): Continuum damage mechanics theory and application, Part II: Application. Int. J. Damage Mech. 7, 274–297.

Appendix A
Theory of Statistical Estimation

Rosenblueth (1975, 1981) developed a useful procedure for determining the moments of a dependent variable in terms of functions of the moments of its independent variables. Rosenblueth's procedure is briefly described in the following.

If F is a function related to random variables $X_1, X_2, \dots, X_n$

$$F = F(X_1, X_2, \dots, X_n). \tag{A1}$$

By definition:

$$\bar{F} = F(\mu_{x_1}, \mu_{x_2}, \dots, \mu_{x_n}), \tag{A2}$$

$$F_{i+} = F(\mu_{x_1}, \dots, \mu_{x_i-1}, \mu_{x_i} + \sigma_{x_i}, \mu_{x_i+1}, \dots, \mu_{x_n}), \tag{A3}$$

$$F_{i-} = F(\mu_{x_1}, \dots, \mu_{x_i-1}, \mu_{x_i} - \sigma_{x_i}, \mu_{x_i+1}, \dots, \mu_{x_n}), \tag{A4}$$

$$\mu(F_i) = \frac{F_{i+} + F_{i-}}{2}, \tag{A5}$$

$$\sigma(F_i) = \frac{F_{i+} - F_{i-}}{2}. \tag{A6}$$

Thus,

$$\mu(F) = \frac{1}{\bar{F}^{n-1}} \prod_{i=1}^{n} \mu(F_i), \tag{A7}$$

$$\sigma^2(F) = \prod_{i=1}^{n} (1 + \sigma^2(F_i)) - 1, \tag{A8}$$

where $\mu(.)$ and $\sigma(.)$ are mean and standard deviation of (.) respectively.

In the case of three variables $F = F(X_1, X_2, X_3)$

$$\mu(F) = \frac{1}{8}(F^{+++} + F^{++-} + \cdots + F^{---}) \tag{A9}$$

$$\sigma^2(F) = \mu(F^2) - \mu^2(F) \tag{A10}$$

where

$$\mu(F^2) = \frac{1}{8}[(F^{+++})^2 + (F^{++-})^2 + \cdots + (F^{---})^2] \tag{A11}$$

$$F^{\pm\pm\pm} = F(\mu_{x_1} \pm \sigma_{x_1}, \mu_{x_2} \pm \sigma_{x_2}, \mu_{x_3} \pm \sigma_{x_3}). \tag{A12}$$

If matrix $[A] = [a_{ij}]$ is a random matrix, then its mean and standard deviation matrices are

$$\mu([A]) = [\mu(a_{ij})] \tag{A13}$$

and

$$\sigma([A]) = [\sigma(a_{ij})]. \tag{A14}$$

According to the above definition,

$$[A]^{\pm} = \mu([A]) \pm \sigma([A]) \tag{A15}$$

where

$$[A]^{\pm} = [a_{ij}^{\pm}] \tag{A16}$$

$$a_{ij}^{\pm} = \mu(a_{ij}) \pm \sigma(a_{ij}). \tag{A17}$$

Authors' address: Prof. Dr. Hong Hao, Department of Civil and Resource Engineering, University of Western Australia, 35 Stirling Highway, Crawley WA 6003, Australia.